Title
TRANSFER PROCESSES IN ECM

Authors
Landolt, D.
Muller, R.H.
Tobias, C.W.

Publication Date
1970-10-01

Presented at the 138th National Meeting of the Electrochemical Society, Symposium on "Fundamental Aspects of Electrochemical Machining," Atlantic City, New Jersey, Oct. 4-9, 1970

UCRL-19615
Preprint c.2

TRANSFER PROCESSES IN ECM

D. Landolt, R. H. Muller, and C. W. Tobias

October 1970

AEC Contract No. W-7405-eng-48

DISCLAIMER

UCRL-19615

TRANSPORT PROCESSES IN ECM

D. Landolt,* R. H. Muller, and C. W. Tobias

Inorganic Materials Research Division, Lawrence Radiation Laboratory,
and Department of Chemical Engineering,
University of California, Berkeley, California

ABSTRACT

ECM is viewed as a special case of an electrochemical process conducted at extremely high current densities with narrowly spaced electrodes. The unusual nature of the process raises questions about the applicability of conventional electrochemical concepts. Particular problems which need clarification include the dynamic behavior of anodic layers and the transport of dissolved, gaseous and solid products from the electrodes. Optical observations, potential measurements and various analytical techniques have been employed to elucidate transport mechanisms involved in the dissolution of copper at current densities up to 150 A/cm^2.

* School of Engineering and Applied Science, University of California, Los Angeles, Calif. 90024

ECM as an Electrochemical Process

ECM is a process in which the complex shape of a tool is reproduced at high speed, with good surface finish, by anodic dissolution of the work piece. From an electrochemical point of view, the process involves electrolysis at very high current densities with small electrode gaps and high electrolyte velocity. Since some of the process parameters of ECM differ by several orders of magnitude from those of conventional electrolysis, it is by no means evident that a simple extrapolation of correlations valid under ordinary conditions can be used for the macroscopic description of ECM. For example, how does overvoltage depend on current density? The activation (charge transfer) overvoltage is often well described by a Tafel line given in Fig. 1. By extrapolating a typical Tafel line, one would expect overvoltages of only a few hundred millivolts, even at the highest ECM current densities.

The ohmic voltage drop in the solution, on the other hand, increases linearly with current density and may reach many volts as shown by the calculated values in Fig. 2. At high current densities, the contribution of the charge transfer overvoltage to the overall cell voltage, therefore, becomes negligible. The linear dependence of the ohmic voltage drop on the current density assumes no effect of hydrogen bubbles or heating on the conductivity. The charge transfer overvoltage values are valid only in the active dissolution regime and do not include concentration overvoltage. When passivation occurs, the voltage balance is drastically altered by a large voltage drop across passivating surface layers. Thermal effects due to the power dissipation in such layers can be expected under these circumstances, the current distribution is likely

to be changed and possible anodic oxygen evolution could decrease current efficiency for the dissolution process.

Another aspect of the process concerns the mass transport from the electrode surfaces. Anodic and cathodic reaction products have to be removed and reactants supplied. Transport of dissolved material by convective diffusion and migration can be described by different dimensionless equations which contain the Nusselt (Nu), Schmidt (Sc) and Reynold's (Re) numbers and depend on the details of the hydrodynamic situation.[3] For the estimation of mass transfer rates in turbulent flow to and from the walls of a rectangular flow channel of hydraulic diameter D_h, the Deissler relation with the Blasius friction coefficient can be used (Eq. 1). For fully developed mass transfer boundary layers* which are independent of the distance from the leading edge of the electrode this can be formulated as

$$Nu = 7.02\times10^{-3}\ Re^{7/8}\ Sc^{1/4} \tag{1}$$

where

$$Nu = \frac{i_l D_h}{zF\Delta cD} \tag{2}$$

$$Re = \frac{vD_h}{\nu} \tag{3}$$

$$Sc = \frac{\nu}{D} \tag{4}$$

i_l = limiting current density

---

* A different equation has to be used for short electrodes on which the mass transfer boundary layer thickness increases in the flow direction (mass transfer entry region).[3]

D_h = hydraulic diameter = 4 times cross section/ perimeter

z = number of electrons transferred per mole

F = Faraday constant

Δc = concentration difference between bulk and electrode surface

D = diffusion coefficient

v = linear flow velocity

ν = kinematic viscosity

A graphic representation of this equation for 3 mm wide electrodes spaced 0.5 mm apart is given in Fig. 3. For the case of a reactant being consumed at the electrode (e.g. in cathodic metal deposition), this relation predicts a maximum rate of discharge when the reactant is depleted at the electrode surface. In anodic metal dissolution, reaction products have to be transported away from the electrode. A maximum possible dissolution rate is due to the finite solubility of reaction products. The concentration driving forces assumed in Fig. 3 for the computations cover the range of poorly to well soluble reaction products. A different transport limitation arises when dissolution results in the formation of complexes. The transport of complexing agent from the solution to the anode may become the limiting factor. An example of this situation is the dissolution of copper in chloride electrolytes where we would expect the dissolution mechanism to depend on the chloride ion concentration.

In the active dissolution mode, the maximum rate of mass transfer can be increased for a given channel geometry by increasing the flow

velocity (Eq. 1). An increased flow velocity results in a decreased thickness δ of the mass transfer boundary layer, which is inversely proportional to the Nusselt number

$$\delta = D_h/Nu \qquad (5)$$

A graphical representation of this relationship for electrodes spaced 0.5 mm apart is given in Fig. 4.

Two questions arise in the extrapolation of transport equations of this type. First, it is not certain that these equations apply to flow fields in narrow gaps. Conventional mass transfer relations have to be modified when the boundary layer thickness becomes comparable to the roughness of the solid surface and cannot be expected to hold when molecular dimensions are reached. Second, we have to ask what happens when the dissolution process is driven at a rate above the limit imposed by convective diffusion and migration. Oxygen evolution would be expected under such conditions. However, there are other possibilities. Supersaturation at the anode could lead to dissolution rates above the predicted limits. If reaction products should be removed from the anode in solid rather than dissolved form, the equations of convective mass transport are not useful for the prediction of limiting phenomena.

Two factors with multiple effects have been neglected so far: cathodic gas evolution and heat dissipation in the solution. Gas evolution affects the electrolyte resistance, resulting in higher cell voltage and possibly different current distribution. Gas may accumulate in large bubbles and lead to two-phase plug flow which drastically affects anodic mass transfer conditions. Gas accumulation on the cathode also

seems to lead to arcing.[4] Cathodic hydrogen may be oxidized at the anode and, thus, decrease the current efficiency for the metal dissolution process. Thermal effects in the solution speed up mass transfer and kinetic processes.

Experimental Considerations

For the study of some of these questions, which have no a priori answers, experiments have been devised to separate the effect of significant electrochemical variables. Due to the particular conditions of electrolysis under ECM conditions (high current density small electrode gap, dissolving anode and high flow velocity), even the simplest electrochemical measurements present major problems.[3,5] A cell design is required which provides for well-controlled high flow velocities at the electrodes and does not involve excessive cell voltages to reach the desired current densities. For example, in order to drive 100 A/cm^2 between two parallel electrodes 2 mm apart, with 1 N KCl solution between them, about 200 volts are required to overcome the ohmic electrolyte resistance. The resulting power dissipation of 100 kW/cm^3 would heat a stagnant electrolyte to the boiling point in 4 milliseconds. The high flow velocities employed in ECM therefore serve two purposes, mass transfer and power dissipation.

Well-defined hydrodynamic conditions can be obtained on rotating disks[6] and cylinders[7] and in flow channels[8]. The latter seems to be most similar to the technical ECM configuration. An experimental flow cell[9] is shown in Fig. 5. Square copper electrodes of 3 × 3 mm surface area are facing each other at a distance of 1 mm. Their separation can be adjusted during the experiment with micrometer screws. Backside

capillaries are provided for the connection of reference electrodes. The downstream capillaries were also used for the sampling of dissolution products. Another cell[3] is shown in Fig. 6. Here, the electrode separation is only 0.5 mm. To insure precise positioning of the electrode surface and reduce edge effects, the electrodes are embedded in epoxy resin. Instead of adjusting the electrode position during dissolution, the duration of each experiment was limited, in order to make changes in electrode spacing negligible. The figure also shows the hydrodynamic entrance length which serves to establish fully developed velocity profiles at the electrodes.

In order to be able to study transport effects, it was decided to keep the chemistry of the dissolution process as simple as possible. Complications, which could be expected due to the complex composition and structure of metals which are technically shaped by ECM, were avoided by the use of copper. This metal has been extensively used for electrochemical studies. It is noble and has relatively well established kinetic and transport properties. It is also easily available in high purity and can easily be prepared in single crystal form. It is realized that the present studies will have to be extended to the dissolution of more complex materials.

Active and Transpassive Dissolution

The simplest electrical measurement which can be made on an electrolytic process consists in establishing a current vs. cell voltage relationship. Some results are shown in Fig. 7. These measurements were obtained by applying a constant current to the cell and measuring the resulting voltage. The approximately linear sections in the curves

near the origin confirm the controlling effect of electrolyte resistance up to a critical current density, where the dissolution switches from the low voltage to a high voltage (transpassive) mode. This transition is moved to higher current densities by an increase in flow velocity. The increase in voltage is more pronounced if one considers the short-time behavior of the electrode because the voltage at constant current exhibits a maximum before reaching steady state as shown in Fig. 8.

Concurrent with the switch from low voltage to high voltage dissolution mode, a change in current efficiency for the dissolution process has been observed.[10] It is shown in Fig. 9. The increase of current efficiency based on two-valent copper above 100% can only be explained by the formation of monovalent copper or the release of metal particles from the electrode surface. The latter explanation would lead one to expect a rough surface and possible grain boundary attack resulting from dissolution in the high voltage mode. Experimental evidence, however, is contrary to this expectation.

Low voltage dissolution of polycrystalline copper in sulfate solution results in a dull, etched surface finish shown in Fig. 10. On the other hand, a bright surface frequently results from high voltage dissolution, Fig. 11. Microscopic examination shows a smooth, randomly pitted surface. Fig. 11 also shows a remnant of an adhering layer of different composition. These layers are likely to introduce a sizeable voltage drop and could, therefore, explain the observed sharp voltage rise. The removal of solid dissolution products from the anode has been proven by sampling the effluent anolyte through a capillary located at the downstream edge of the anode. The composition of solids

thus collected, formed in sulfate and nitrate solution, has been analyzed by x-ray diffraction techniques. Their main constituent was cuprous oxide. The power dissipation due to the electrical resistance of the layers results in the release of large quantities of heat at the electrode. It is possible that thermal effects are responsible for voltage fluctuations such as the ones shown in Fig. 12. Optical observation in chlorate electrolyte showed that the periodic formation and removal of surface layers goes parallel to the voltage fluctuations and is associated with similar temperature fluctuations. Further evidence for the anodic origin of the voltage fluctuations is contained in Fig. 12, which shows that the anode potential fluctuations (measured vs. a saturated calomel electrode) parallel the cell voltage fluctuations, while the cathode potential stays reasonably constant. It should be pointed out that these potential measurements can be used only in a qualitative sense because they contain a large ohmic component which results from the finite distance between reference capillary and electrode surface, and were measured with only 100 kΩ input impedance.

Cathodic Gas Evolution

In addition to cell voltage oscillations due to anode processes, cathodic gas evolution can also lead to voltage fluctuations. Such a case is illustrated in Fig. 13. Typically, these oscillations are much more irregular than the anodic ones. They result from the formation of large gas bubbles in the inter-electrode gap illustrated in Fig. 14. Upon further reduction of electrolyte velocity or increase in current density, arcing may occur.

Another effect of gas bubbles released from the cathode is an

increase of the ohmic resistance of the electrolyte. This increase results in an increased cell voltage under controlled current conditions. Fig. 15 illustrates this effect for two different current densities.[4] It can be seen that the voltage increases sharply upon reducing the flow rate below a certain value. The dotted lines indicate the range of voltage fluctuations.

Transport Limitations

For copper dissolution in sulfate and nitrate solution, the onset of transpassive behavior roughly coincides with the limiting rate of transport for reaction products in dissolved form.[3] The voltage step due to this anodic transport limitation is independent of the voltage rise (and instability) due to cathodic transport limitations.

In the transpassive dissolution mode, the ohmic resistance of the surface layer leads to a re-distribution of current density over the electrode face. A controlling ohmic resistance at the electrode surface counteracts the effect of different voltage drops in the electrolyte to different locations on the anode surface and, thus, results in a more uniform current distribution. The polished surface finish, observed to result from transpassive dissolution, may be due to the equalizing effect of surface layers on a microscopic scale.

If the presence of passivating layers is desirable in ECM, then it becomes important to form such layers in a controlled way and to continue the dissolution process despite their presence. Different modes of transport can be postulated under these circumstances. Dissolution products could move by ionic migration or diffusion through the solid layer and in pores of the film. Alternately, the solid layer could

be formed and shed periodically. Such behavior seems to be most pronounced in chlorate solution and may be a reason for the desirable properties of this electrolyte. Since in the transpassive dissolution regime, reaction products have to be removed from the anode surface faster than can be accounted for by convective diffusion of dissolved material, a transport of solid reaction products must be postulated. Dissolution experiments have been conducted at current densities ten times the current density at which transpassive behavior sets in. Under these conditions, 90% of the reaction products appear to be removed from the anode in solid form. A satisfactory quantitative description of the transport of solids under these circumstances is not available. Optical observations have shown that at high flow velocities, the solids are finely divided and may be difficult to detect. At low flow rates or in stagnant solutions, however, their formation can be visibly demonstrated. A color motion picture which illustrates the sequence of precipitate formation and removal in continued electrolysis has been prepared.*

Acknowledgment: This work was conducted under the auspices of the U. S. Atomic Energy Commission.

---

* Presented at the symposium.

REFERENCES

1. E. Mattson, J. O'M. Bockris, Trans. Faraday Soc. 55, 1586 (1959).
2. K. Vetter, Elektrochemische Kinetik, Springer Verlag, Berlin, 1961, p. 432.
3. D. Landolt, R. H. Muller, C. W. Tobias, J. Electrochem. Soc. 116, 1384 (1969).
4. D. Landolt, R. Acosta, R. H. Muller, C. W. Tobias, J. Electrochem. Soc. 117, 839 (1970).
5. D. Landolt, R. H. Muller, C. W. Tobias, J. Electrochem. Soc., submitted.
6. V. G. Levich, Physicochemical Hydrodynamics, Prentice-Hall, Inc. Englewood Cliffs, N. J., 1962, p. 60.
7. M. Eisenberg, C. W. Tobias, C. R. Wilke, J. Electrochem. Soc. 101, 306 (1954).
8. R. G. Hickman, C. W. Tobias, Z. Physik. Chem. 229, 145 (1965).
9. K. Kinoshita, Ph. D. Thesis, University of California, Berkeley, UCRL-19051, Sept. 1969.
10. K. Kinoshita, D. Landolt, R. H. Muller, C. W. Tobias, J. Electrochem. Soc., 117, 1246 (1970).

FIGURES

Fig. 1. Tafel lines for the charge transfer overvoltage of anodic copper dissolution[1] and cathodic hydrogen evolution on copper.[2]

Fig. 2. Total charge transfer overvoltage and ohmic voltage drop calculated for active copper dissolution and cathodic hydrogen evolution in a 2 M KNO_3 electrolyte with electrodes spaced 0.5 mm apart.

Fig. 3. Limiting current densities predicted by the Deissler relation for ionic mass transport from parallel electrodes spaced 0.5 mm apart for concentration differences Δc of 10, 1 and 0.1 moles/liter between interface and bulk solution. (Numerical values used $D=10^{-5}$ cm^2/sec, $\nu=10^{-2}$ cm^2/sec, $z=2$.)

Fig. 4. Calculated thickness δ of mass transfer boundary layer for same conditions as in Fig. 3.

Fig. 5. Experimental flow cell with electrodes of 3 × 3 mm surface area, electrode separation 1 mm.

Fig. 6. Experimental flow cell with electrodes 0.5 × 3 mm (or 2 mm round), electrode separation 0.5 mm.

Fig. 7. Current density and cell voltage for electrolysis in 1 M K_2SO_4 with copper electrodes spaced 0.5 mm apart. Flow velocity 100 and 400 cm/sec. Initial, peak and steady state voltages as defined in Fig. 8.

Fig. 8. Typical oscillograph traces of cell voltage U, apparent anode potential e_A, current density i and apparent cathode potential e_C for transpassive dissolution of copper at constant current showing initial, peak and steady state voltage values.

0.2M K_2SO_4, 400 cm/sec, 50 A/cm^2, electrode separation 0.5 mm.

Fig. 9. Current efficiency for copper dissolution in 0.5 M K_2SO_4 based on the formation of Cu^{++}. Flow velocity 50 cm/sec and 686 cm/sec, electrode separation 1 mm.

Fig. 10. Etched surface of copper after active dissolution. 0.2 M K_2SO_4, 2500 cm/sec, 20 A/cm^2, electrode separation 0.5 mm.

Fig. 11. Bright, pitted surface of copper after transpassive dissolution. 0.2 M K_2SO_4, 1000 cm/sec, 20 A/cm^2, electrode separation 0.5 mm. Remnant of passivating surface layer on the left.

Fig. 12. Cell voltage fluctuations due to anodic processes. U-cell voltage, e_A-apparent anode potential, i-current density, e_C-apparent cathode potential. 0.2 M K_2SO_4, 400 cm/sec, 20 A/cm^2, electrode separation 0.5 mm.

Fig. 13. Cell voltage fluctuations due to cathodic processes. Symbols as in Fig. 12. 0.2 M K_2SO_4, 100 cm/sec, 50 A/cm^2, electrode separation 0.5 mm.

Fig. 14. Formation of cathodic gas patches associated with cathodic potential fluctuations. High-speed photograph, 2 M KCl, 400 cm/sec, 100 A/cm^2, electrode separation 0.5 mm. Cathode facing up, flow from right to left.

Fig. 15. Effect of cathodic gas evolution on cell voltage at constant current density. 2 M KCl, electrode separation 0.5 mm, •-cathode facing down, o-cathode facing up, --- amplitude range of voltage fluctuations.

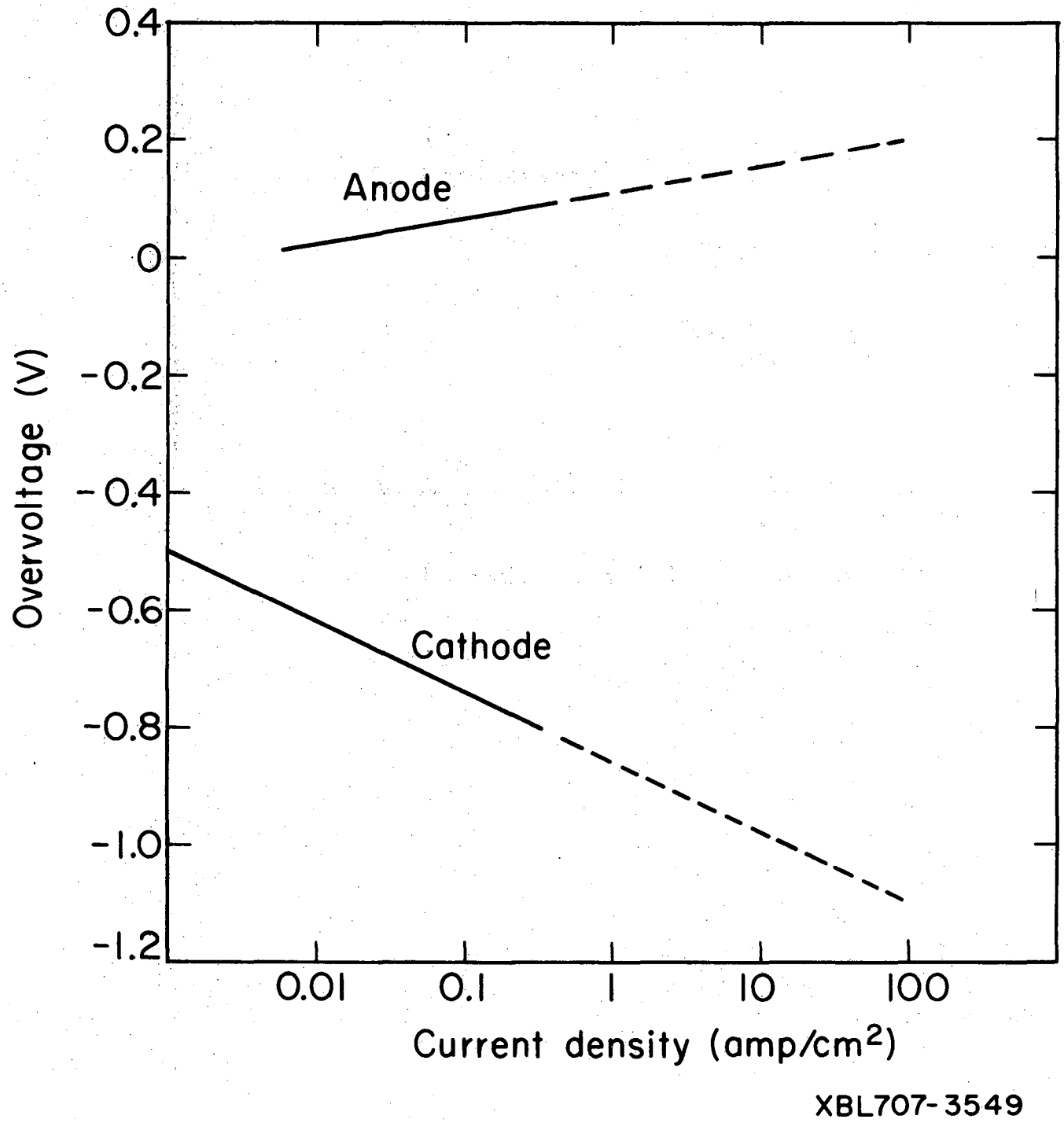
0.4
0.2
0
-0.2
-0.4
-0.6
-0.8
-1.0
-1.2
Overvoltage (V)
Anode
Cathode
0.01
0.1
1
10
100
Current density (amp/cm²)
XBL707-3549

Fig. 1.

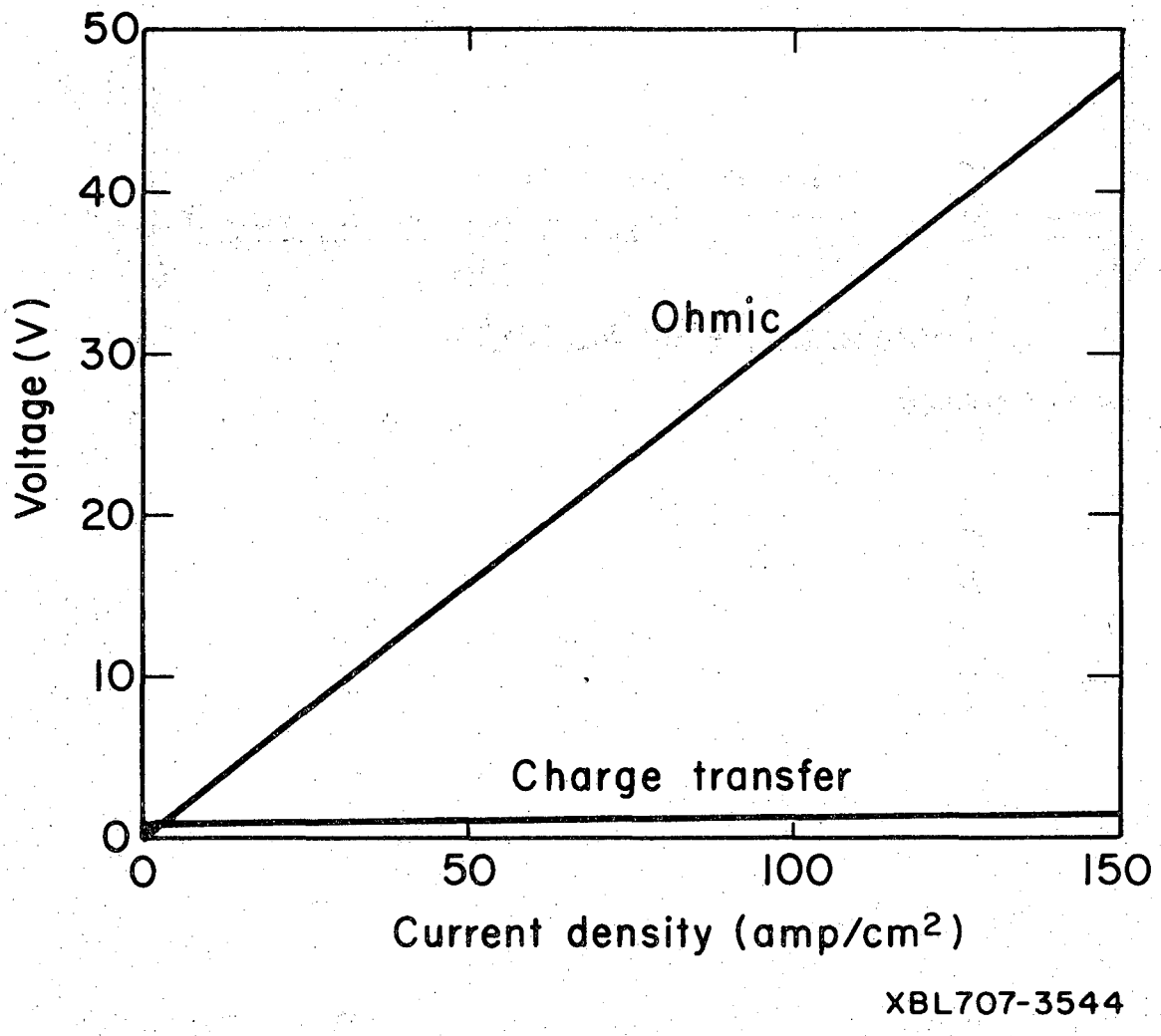
50
40
30
20
10
0
Voltage (V)
Ohmic
Charge transfer
0
50
100
150
Current density (amp/cm²)
XBL707-3544

Fig. 2.

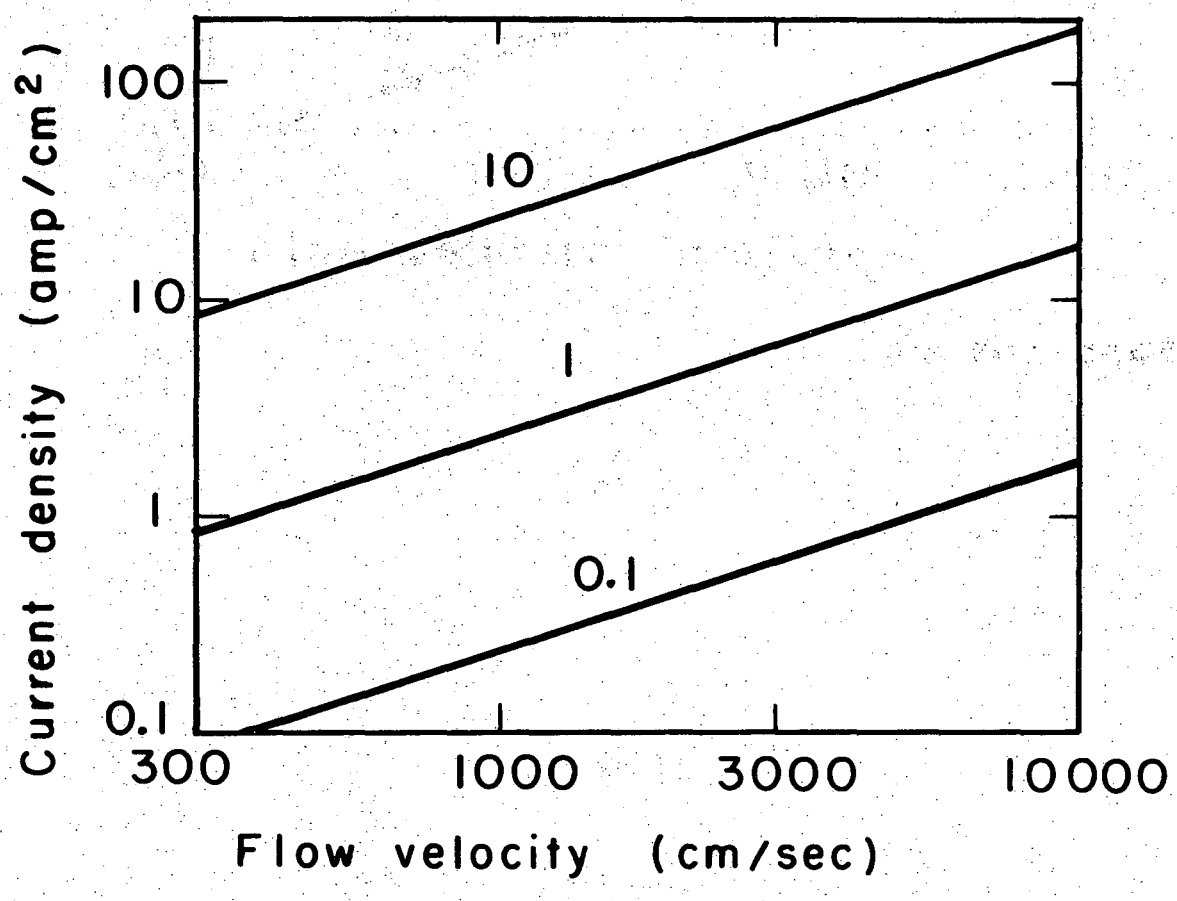
Current density (amp/cm²)
100
10
1
0.1
10
1
0.1
300
1000
3000
10000
Flow velocity (cm/sec)
XBL707-3545

Fig. 3.

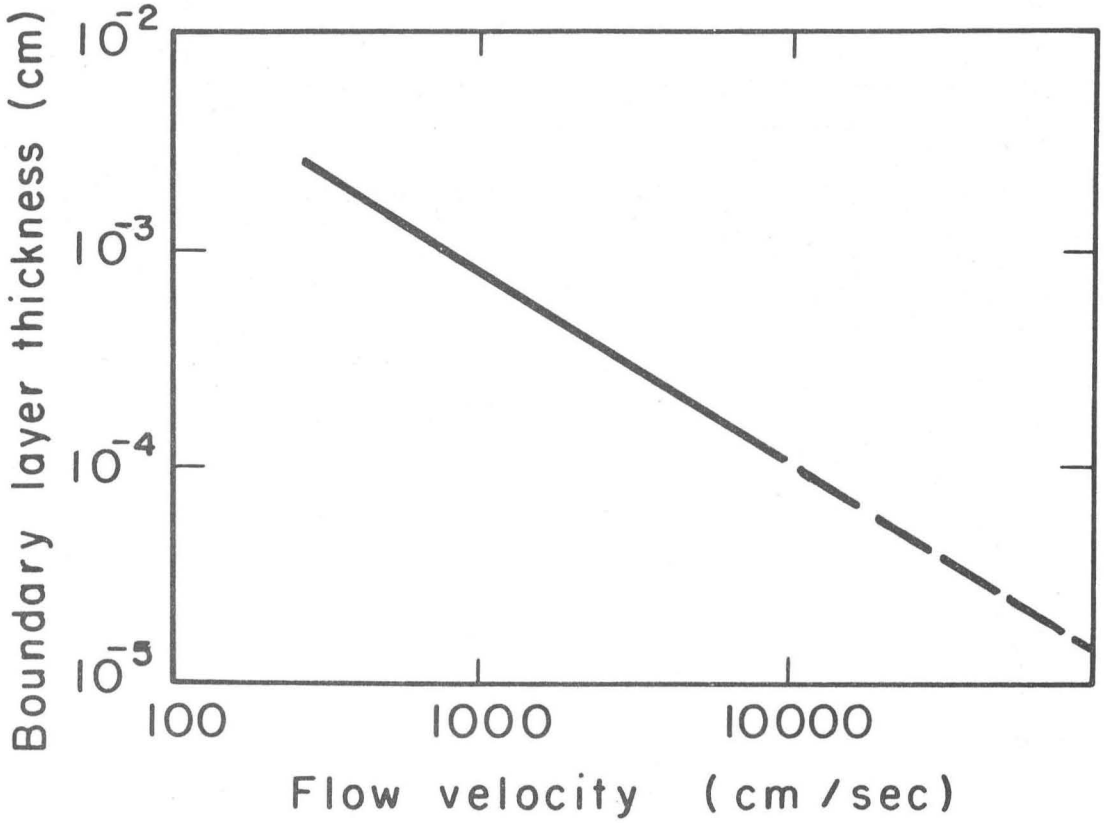

XBL707-3543

Fig. 4.

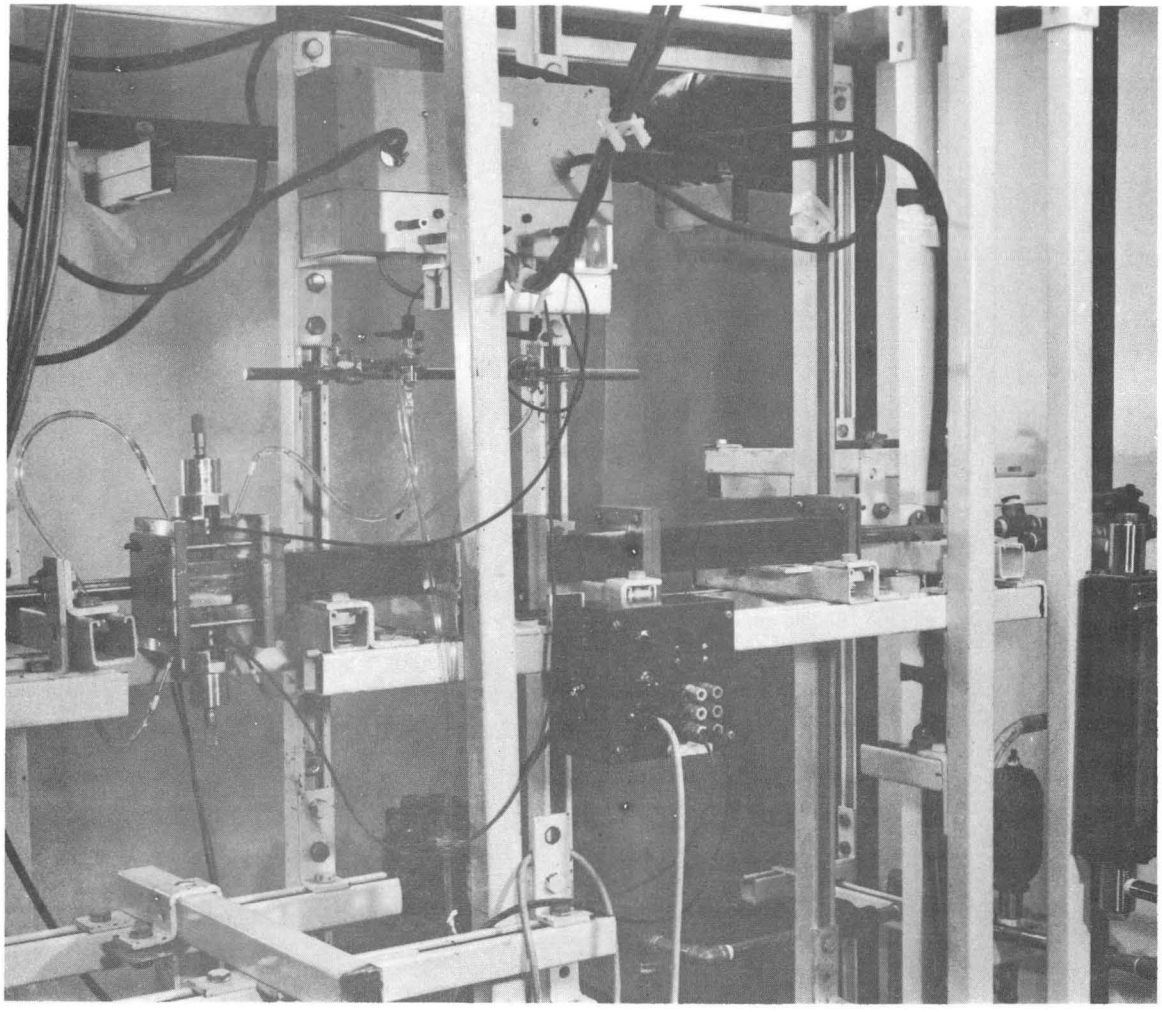

XBB688-5010

Fig. 5.

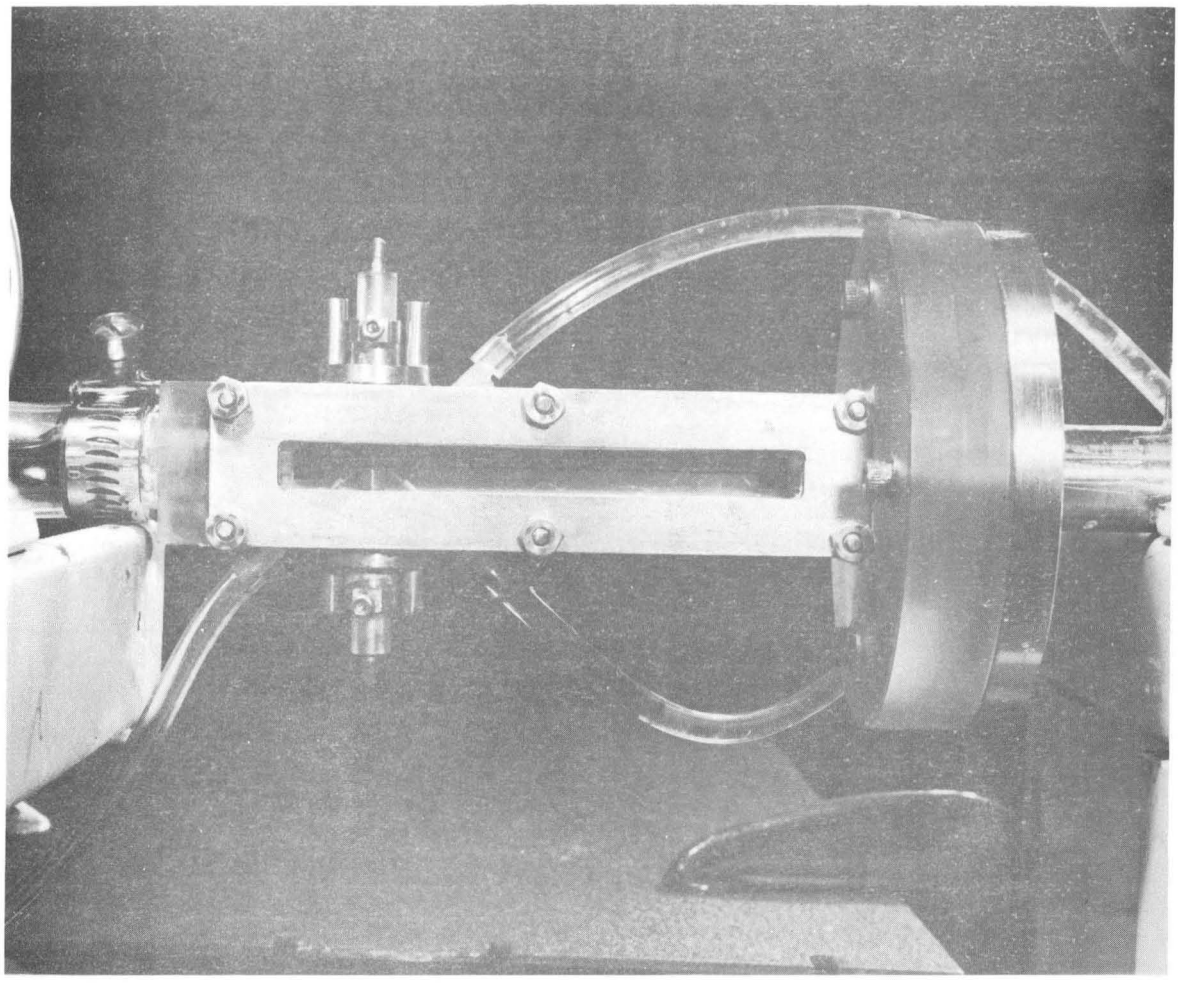

CBB6712-7050

Fig. 6.

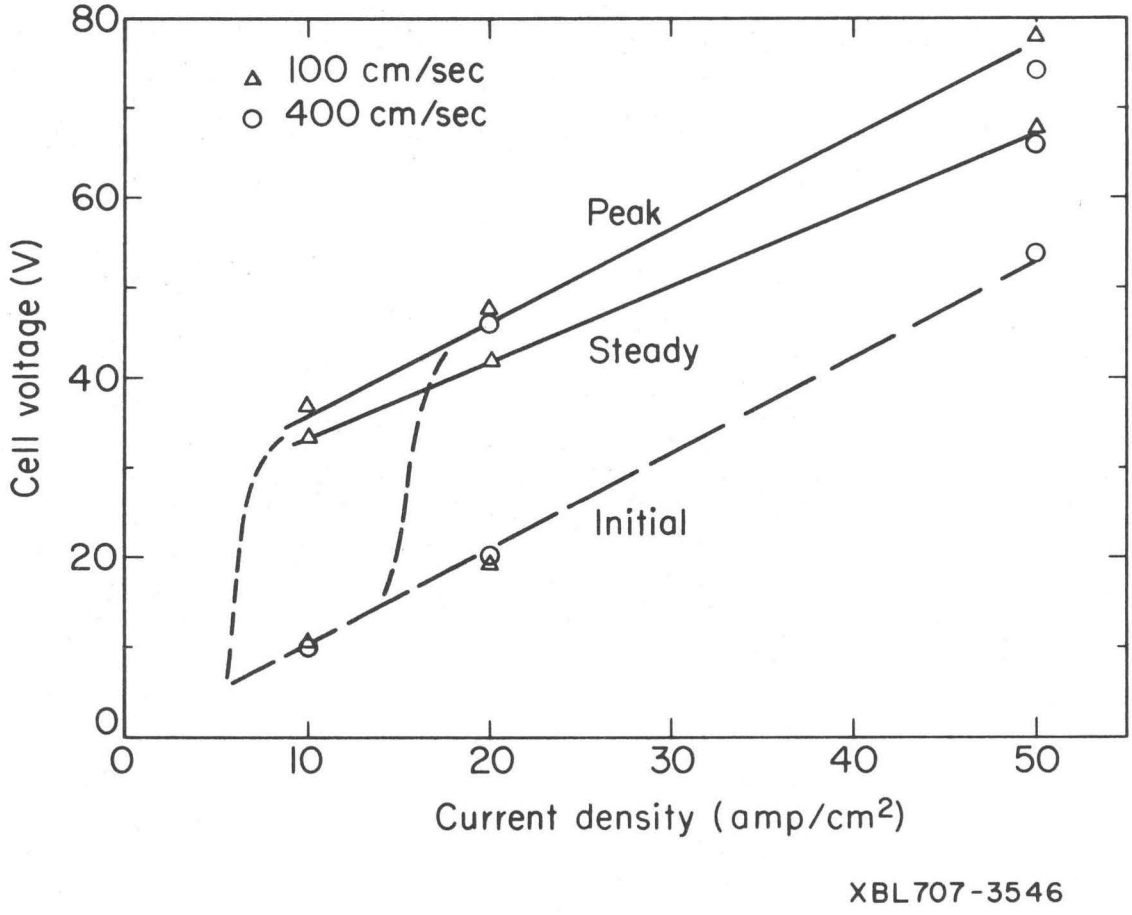
80
60
40
20
0
0
10
20
30
40
50
Cell voltage (V)
Current density (amp/cm²)
△ 100 cm/sec
○ 400 cm/sec
Peak
Steady
Initial
XBL707-3546

Fig. 7.

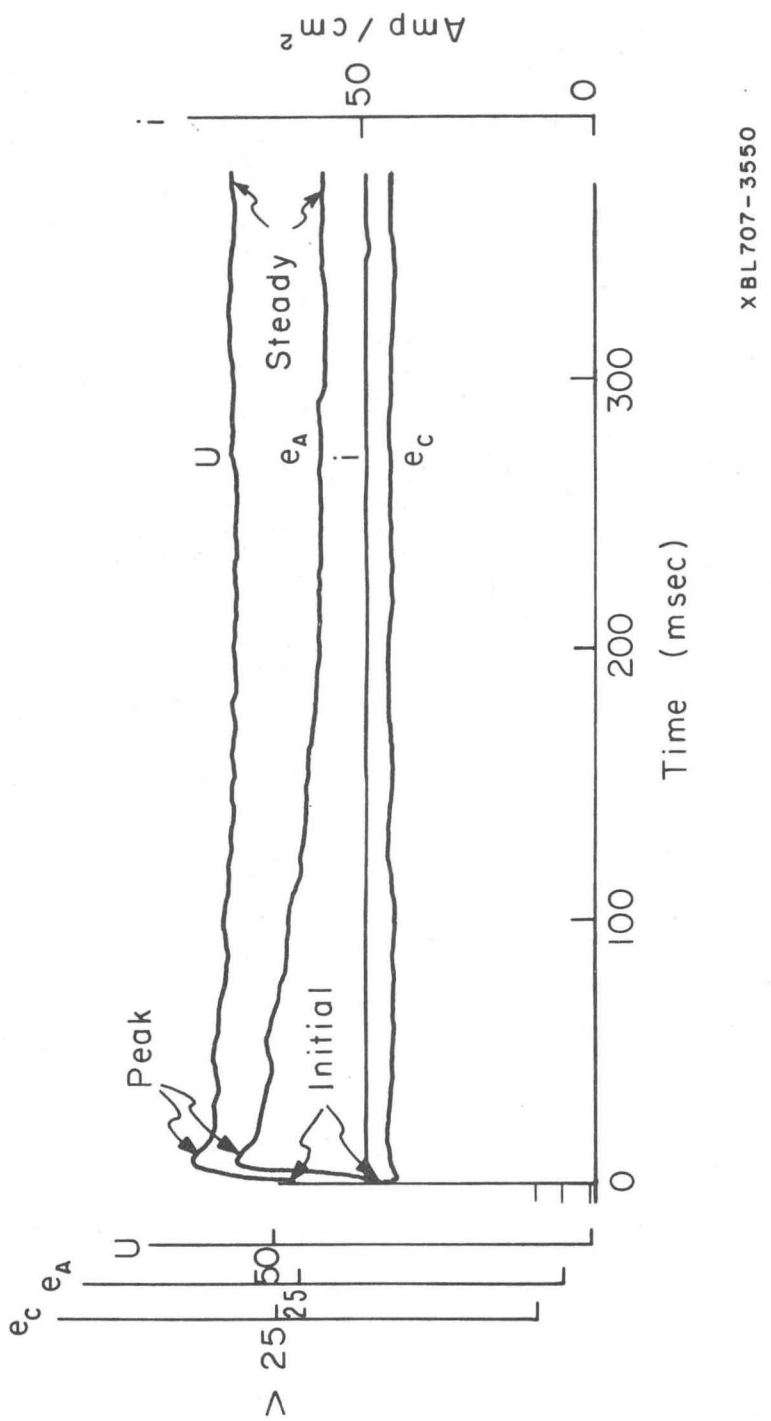

XBL707-3550

Fig. 8.

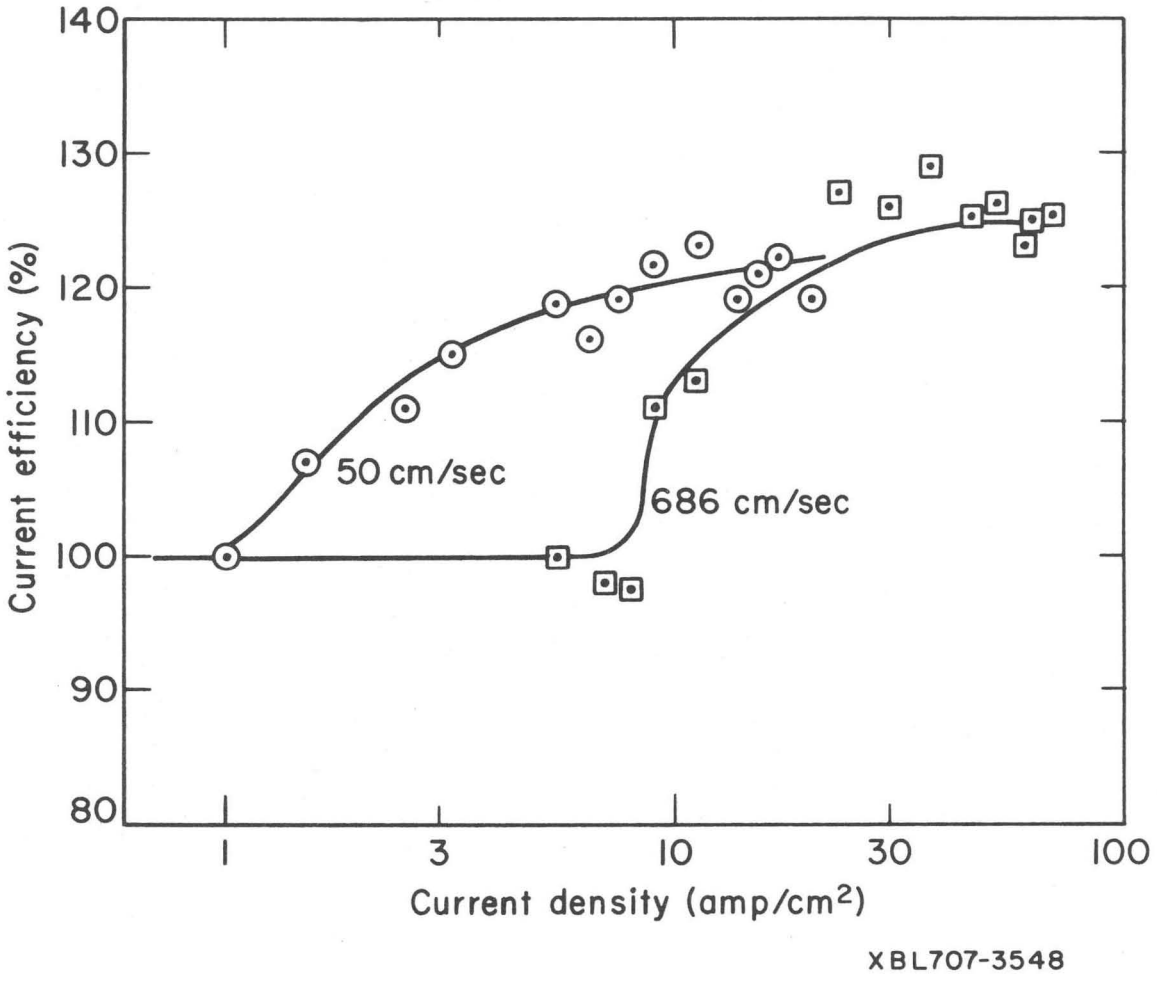
140
130
120
110
100
90
80
Current efficiency (%)
50 cm/sec
686 cm/sec
1
3
10
30
100
Current density (amp/cm²)
XBL707-3548

Fig. 9.

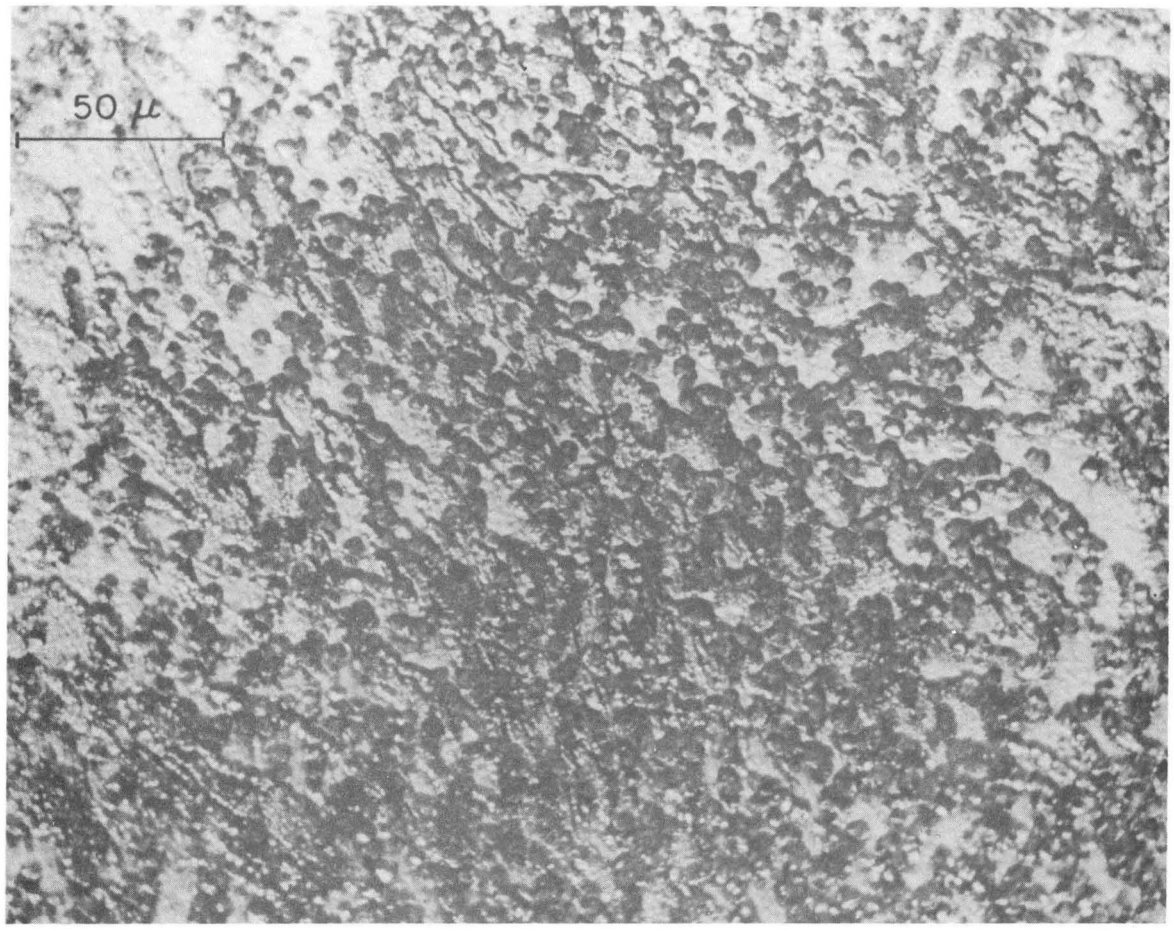

XBB707-3383A

Fig. 10.

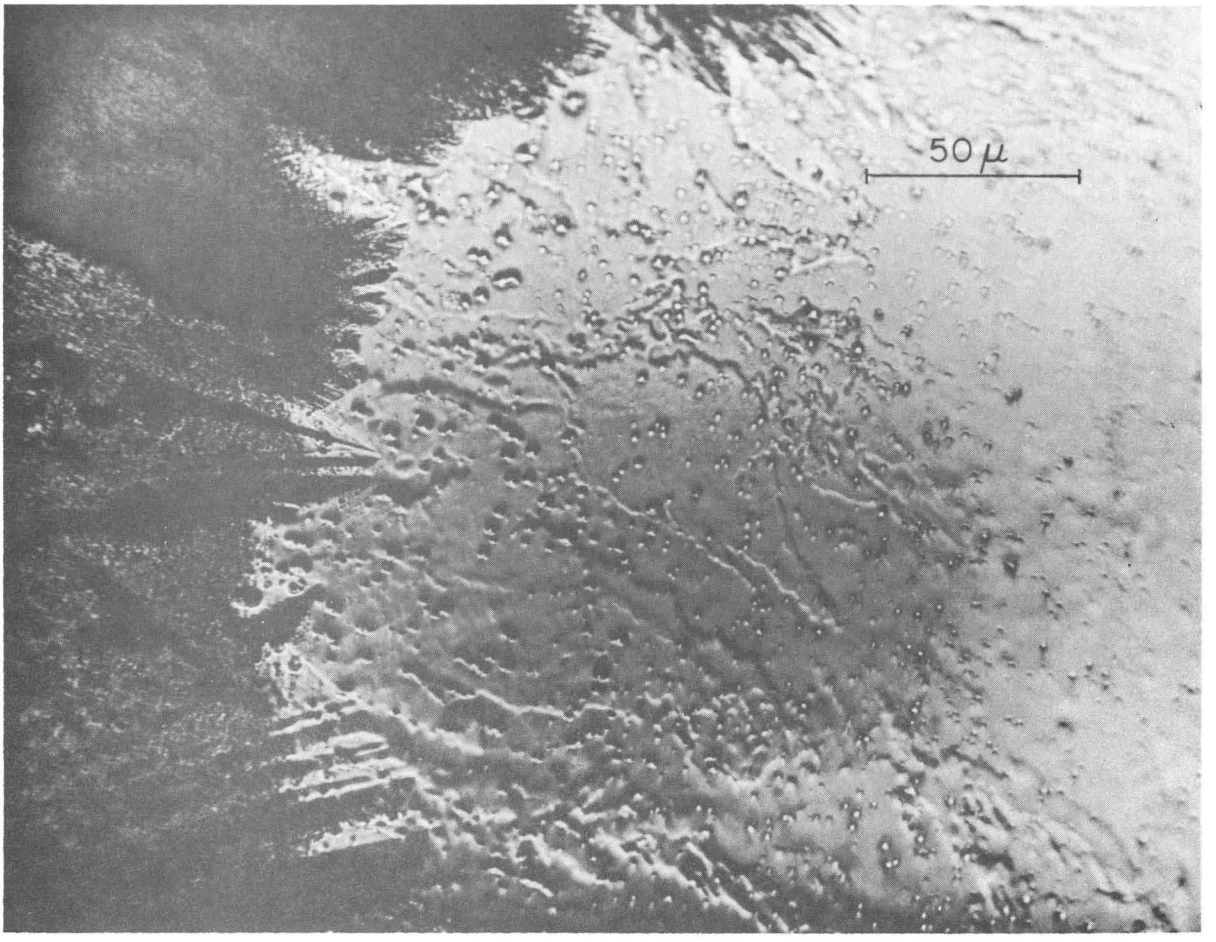

XBB709-4270

Fig. 11.

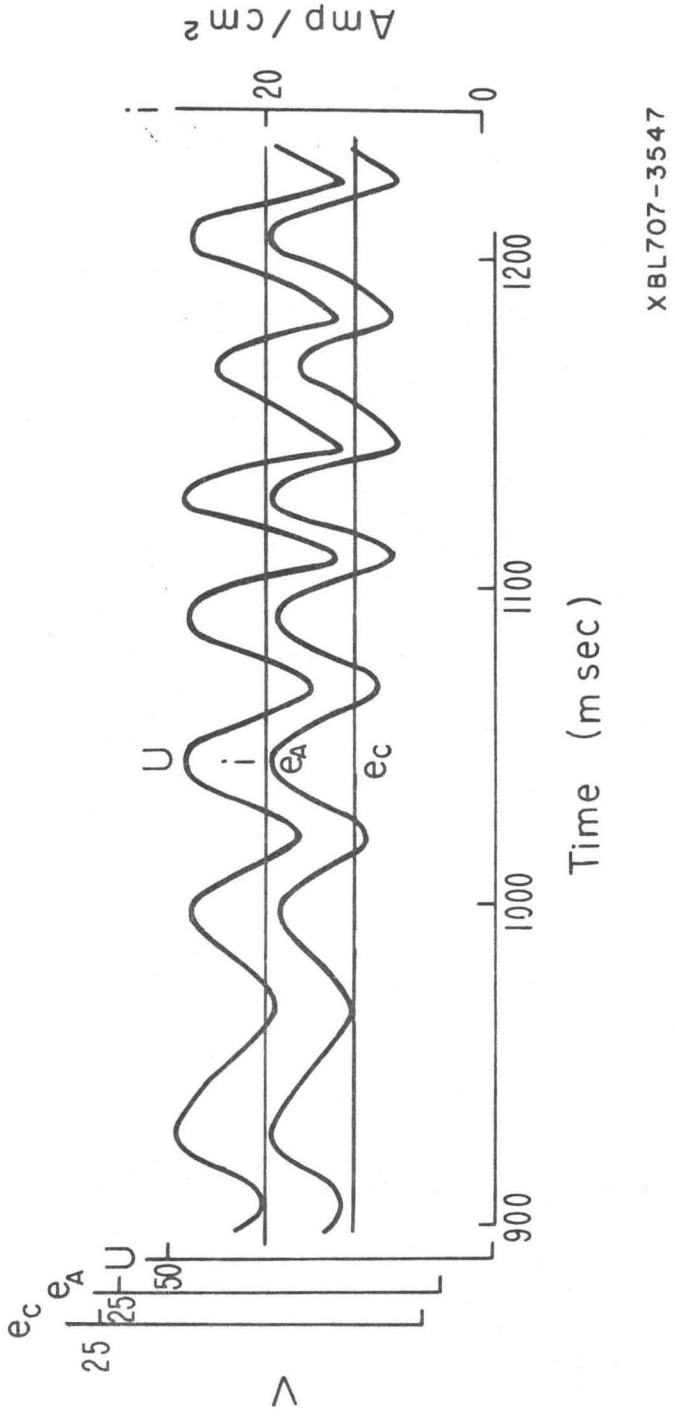

XBL707-3547

Fig. 12.

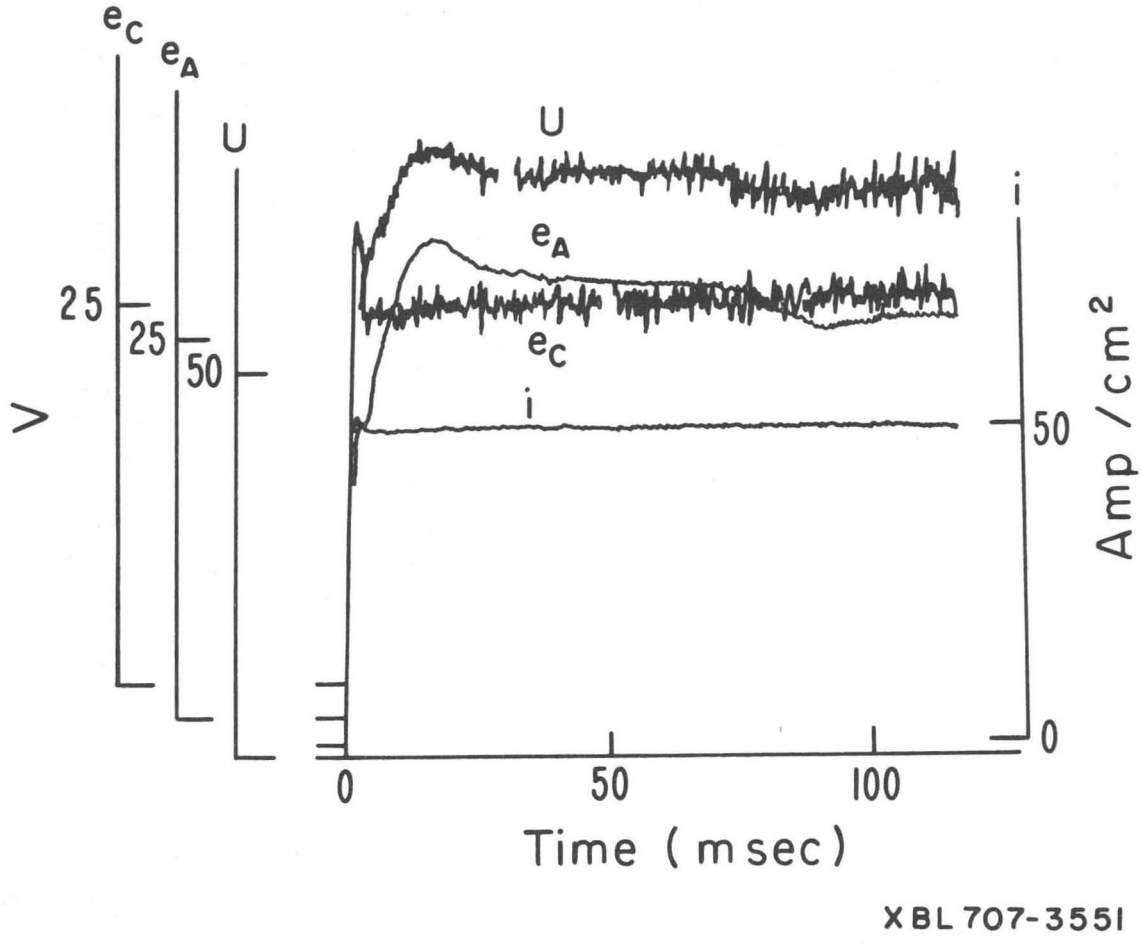
e_C
e_A
U
25
25
50
V
U
e_A
e_C
i
i
50
0
Amp / cm²
0
50
100
Time (msec)
XBL 707-3551

Fig. 13.

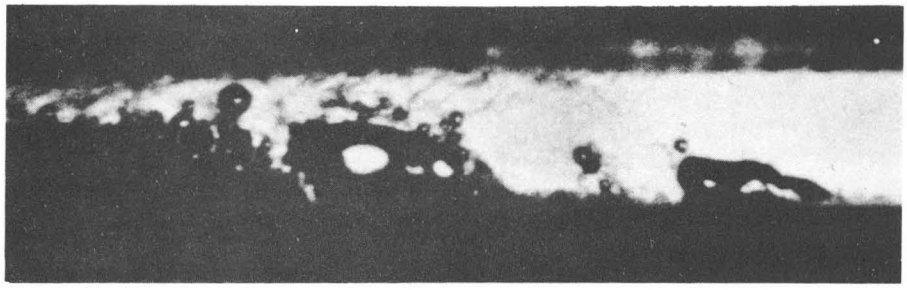

XBB699-5796A

Fig. 14.

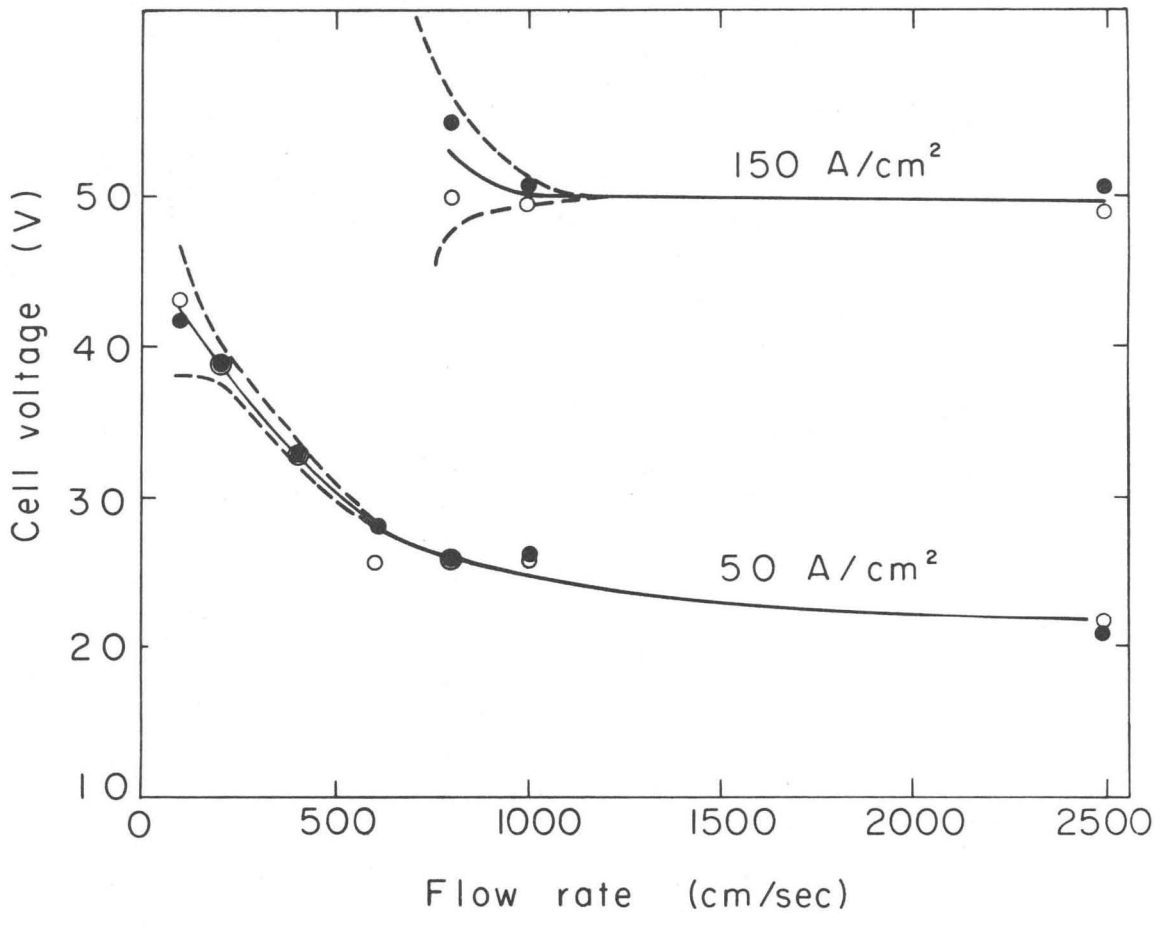

XBL 698-3571-A

Fig. 15.

TECHNICAL INFORMATION DIVISION
LAWRENCE RADIATION LABORATORY
UNIVERSITY OF CALIFORNIA
BERKELEY, CALIFORNIA 94720